Hindawi
Advances in Meteorology
Volume 2018, Article ID 2469156, 14 pages
https://doi.org/10.1155/2018/2469156

Research Article

Drought Propagation Patterns under Naturalized Condition Using Daily Hydrometeorological Data

Jianzhu Li,[1] Yuangang Guo,[1] Yixuan Wang,[1,2] Shanlong Lu,[3] and Xu Chen[1]

[1]*State Key Laboratory of Hydraulic Engineering Simulation and Safety, Tianjin University, Tianjin, China*
[2]*College of Water Conservancy and Civil Engineering/Inner Mongolia Water Resource Protection and Utilization Key Laboratory, Inner Mongolia Agricultural University, Hohhot, China*
[3]*Institute of Remote Sensing and Digital Earth, Chinese Academy of Sciences, Beijing, China*

Correspondence should be addressed to Yixuan Wang; wjxlch@tju.edu.cn

Received 10 May 2018; Revised 12 August 2018; Accepted 28 August 2018; Published 8 October 2018

Academic Editor: Francesco Viola

Drought propagation pattern forms a basis for establishing drought monitoring and early warning. Due to its regional disparity, it is necessary and significant to investigate the pattern of drought propagation in a specific region. With the objective of improving understanding of drought propagation pattern in the Luanhe River basin, we first simulated soil moisture and streamflow in naturalized situation on daily time scale by using the Soil and Water Assessment Tool (SWAT) model. The threshold level method was utilized in identifying drought events and drought characteristics. Compared with meteorological drought, the number of drought events was less and duration was longer for agricultural and hydrological droughts. The results showed that there were 3 types of drought propagation pattern: from meteorological drought to agricultural/hydrological drought (M-A/H), agricultural/hydrological drought without meteorological drought (NM-A/H), and meteorological drought only (M). To explain the drought propagation pattern, possible driven factors were determined, and the relations between agricultural/hydrological drought and the driven factors were built using multiple regression models with the coefficients of determination of 0.4 and 0.656, respectively. These results could provide valuable information for drought early warning and forecast.

1. Introduction

Drought is a complicated, recurrent natural hazard with characteristics of covering extensive areas and lasting for months to years [1, 2], which have significant negative impacts on economy and ecology [3–6]. Drought is commonly defined as a persistent occurrence of below-normal natural water availability [7], which is applicable to each part of the terrestrial hydrological cycle. In general, drought is distinguished into different types related to components of hydrological cycle: meteorological drought (a precipitation deficit), agricultural or soil moisture drought (a below-normal storage in the unsaturated zone), hydrological drought (water availability lower than the normal in aquifers and/or streams), and socioeconomic drought (occurring when the demand of various commodities for water exceeds the supply) [8].

Drought starts with periods of precipitation deficit and propagates through the terrestrial hydrological system, which in turn results in drought in soil moisture and groundwater or streamflow [7, 9]. The developing process is called drought propagation. The term "drought propagation" was introduced as a theoretical framework by Changnon [10], nevertheless, created as a term by Eltahir and Yeh [11]. Precipitation deficit with a prolonged period decreases streamflow, subsurface water and groundwater storage, and generated hydrological drought [12, 13]. Based on Van Loon [14], the features of drought propagation include lag, lengthening, attenuation, and pooling. Hisdal and Tallaksen [3] showed streamflow droughts are less frequent and more persistent than precipitation droughts. Van Lanen [15] demonstrated propagation of recharge drought led to slighter hydrological drought in different climate regions.

In previous studies, it was demonstrated that drought propagation was affected by climate seasonality [13, 16–18]. Sung and Chung [13] pointed that streams with lower than the average discharge during high-stream seasons might affect drought development. Huang et al. [16] examined the propagation time from meteorological to hydrological drought using the cross wavelet analysis, and found the propagation time has seasonality with short time in spring and summer and long duration in autumn and winter. Based on drought propagation processes in different seasons, Van Loon and Van Lanen [18] divided hydrological drought into six types, which resulted from interaction of precipitation and temperature in various seasons. Van Loon et al. [17] revealed that how seasonality of climate influenced drought propagation.

The key steps of drought propagation studies are to identify drought event and define the characteristics of drought events. Drought frequency (Number of drought events) and severity (drought duration and deficit volume) are vital features to define characteristics of drought events, which can reflect translation of drought signals in a hydrological system [7, 19, 20]. Tallaksen et al. [20] showed deficit volume was a robust feature to weigh on the severity of drought event over the catchment area. Many studies have concentrated on defining drought and drought characteristics using various indices, which include Standardized Precipitation Index (SPI), Standardized Streamflow Index (SSI), Standardized Precipitation Evapotranspiration Index (SPEI), and Standardized Runoff Index (SRI) [16, 21, 22].

Apart from indices, the above-mentioned drought features also can be obtained by the threshold level method. The threshold level method can truncate continuous time series with a defined threshold value, and it includes fixed and variable threshold. Variable threshold, changing over the year, reflects the seasonality, which has been widely applied to the study of drought propagation [7, 23–27]. Compared with drought indices, threshold level method can calculate deficit volume, which is an important feature in water management. It does not require a preferred knowledge of probability distributions [21]. On the other hand, all drought categories of hydrometeorological variables can make comparison by threshold level method, which is necessary when studying drought propagation. It has been testified that this method has a potential capacity to analyze daily-based drought [19, 28, 29].

In order to analyze drought propagation including agricultural drought and groundwater drought, hydrological models are usually applied, such as the conceptual, semi-distributed rainfall-runoff model-HBV [14, 19], combined SWAP and MODFLOW models [30], and spatially distributed physically based model SIMGRO [15]. These models were employed to simulate the soil moisture and groundwater time series, which cannot be observed directly. In regions where human activities affect runoff processes, hydrological models are essential to distinguish the naturalized and human-induced drought.

In this study, the primary objectives are (1) to investigate drought propagation patterns on daily scale with naturalized situations (without human effect) and (2) to explain the driven factors that affect drought propagation in the Luanhe River basin.

2. Study Area

The Luanhe River basin is located in the northeast part of China, which is between 115°30′E~119°15′E and 39°10′N~42°30′N (Figure 1). The Luanhe River originates from Mongolia Plateau, passes through the Yanshan Mountains, and eventually flows into the Bohai Bay with a total drainage area of 44600 km^2. There are three geographic types in the basin, which are plain, mountains, and plateaus. The altitude ranges from 2 to 2205 m with an average of 766 m.

The basin belongs to temperate semiarid continental monsoon climate with cold winter and hot summer. Annual average temperature is −0.3~11°C. Annual potential evaporation is 950~1150 mm. Average annual precipitation is 535 mm, with 70%~80% of annual rainfall in the flood season (June–September). This attributes to unstable characteristics of the duration, intensity, and location of the subtropical high over the northern Pacific in summer [31]. The Luanhe River basin has a strong seasonality in meteorological forcing, with relatively low precipitation and low potential evapotranspiration in winter and spring and relatively high precipitation and high potential evapotranspiration in summer. This results in a strong seasonality in discharge. Highest river flows occur in summer and the low-flow season is winter.

Luanhe River basin suffered from severe droughts in 1972, 1980–1984, and 1997–2005. The annual runoff in this basin showed significant decreasing trend and resulted in a long hydrological drought during last decade, which affected the water supply to Tianjin and Tangshan cities. Therefore, it is of great significance to select Luanhe River basin as the study area to research drought propagation.

3. Data

For the study area, daily rainfall data were available from 13 rain gauges and 5 weather stations inside or around the basin during 1963~2012. Daily streamflow data ranging from 1963 to 2012 were available at Luanxian station, which controlled 98.2% of the Luanhe River basin. The data from 13 rain gauges and Luanxian station were provided by Hydrology and Water Resource Survey Bureau of Hebei Province. Rainfall from the 5 weather stations and other meteorological data (wind, temperature, humidity, etc.) was downloaded from China Meteorological Data Service Center (CMDC) (http://data.cma.cn).

Geospatial data were also required in SWAT model such as DEM (digital elevation data) with resolution of 30 m∗30 m, land use and soil data. DEM was downloaded from the website of Geospatial Data Cloud (http://www.gscloud.cn/). Remotely sensed land use data of 1970 were provided by the Chinese Academy of Sciences. Soil data were available from China Soil Map Based Harmonized World Soil Database (v1.1) [32, 33].

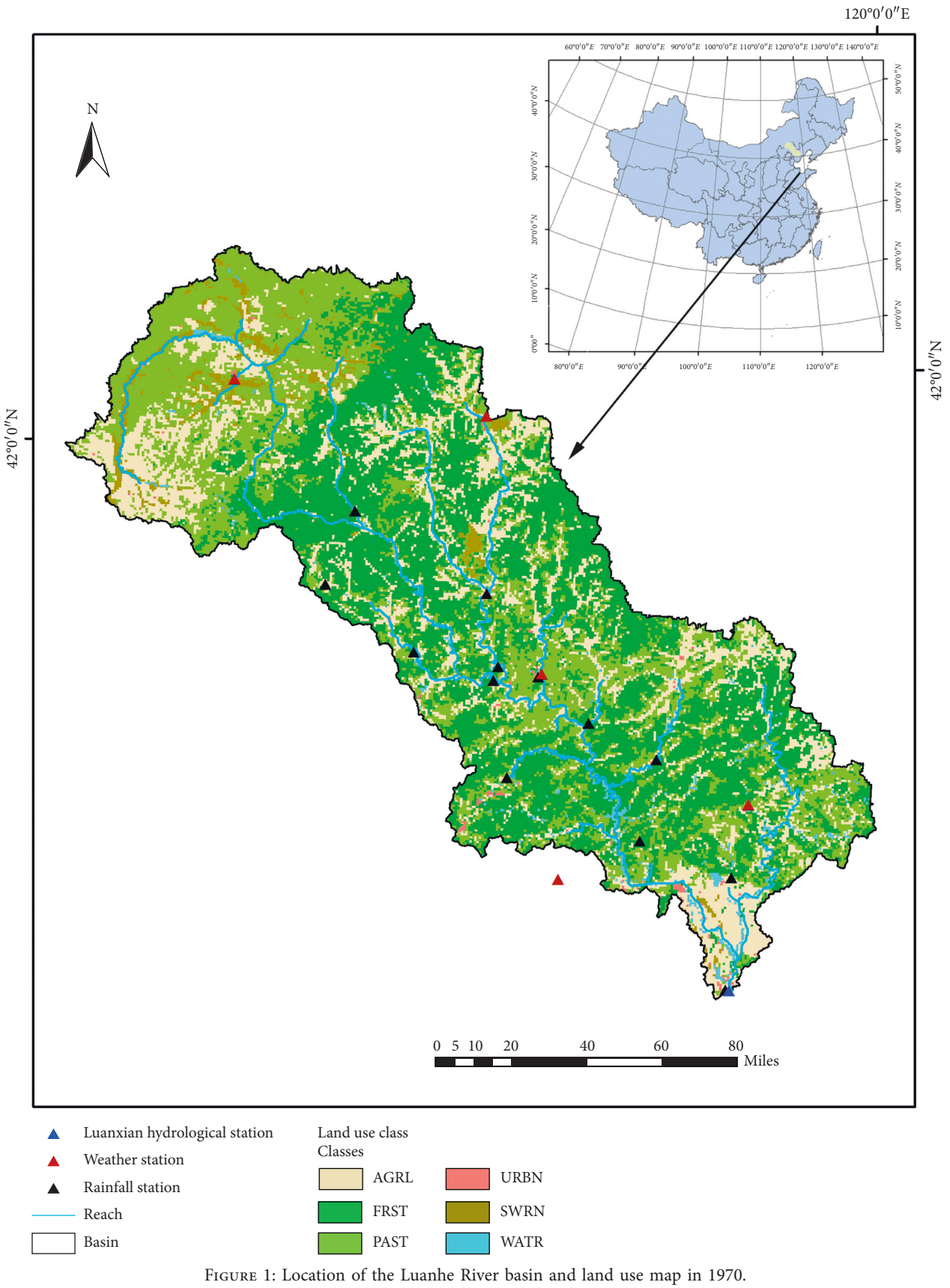

Figure 1: Location of the Luanhe River basin and land use map in 1970.

4. Methods

4.1. Identification of Temporal Change in Hydrological Series. In order to investigate the validity of stationarity assumption for precipitation records over the Luanhe River basin, temporal changes in observed precipitation series were identified by traditional statistical approaches.

4.1.1. Identification of Temporal Trends. Mann-Kendall (MK) trend test [34, 35] is one of the mostly widely applied nonparametric tests for trend detection in hydrologic time series. Before employing the MK trend test, the trend-free prewhitening (TFPW) procedure proposed by Yue et al. [36] is usually used to efficiently eliminate the influence of serial correlation on the MK test.

For identifying the true slope of MK trend analysis, the Sen's slope estimator developed by Sen [37] is commonly adopted [38, 39]. The Sen's produce applied following the MK test measures the magnitude of any significant trend found in the MK test.

In this study, the MK trend test with TFPW procedure and Sen's method were used to determine the temporal trends in precipitation. Details of the three methods can be found in Kisi and Ay [40]; Yue et al. [36], and Da Silva et al. [41] respectively.

4.1.2. Identification of Change Points. There are many methods to determine the change point of hydrological series, such as moving F test method [42], R/S analysis method [43], and Bayesian model [44].

The nonparametric Mann–Kendall–Sneyers test [34, 35, 45] was applied in this study to determine the occurrence of a change point. This test is widely used to detect abrupt change in hydrological data, because it has the advantage of not assuming any distribution form for the data and has similar power to its parametric counterparts. The normalized variable statistic UF_k of the forward sequence and UB_k of the backward sequence are calculated and used to plot the forward and backward curves. If the intersection of the two curves occurs within the given confidence interval, then it indicates a change point.

In addition, the nonparametric Pettitt test developed by Pettitt [46] was further employed in this study to examine the change points obtained by the Mann–Kendall–Sneyers test. The Pettitt test detects a significant change in the mean value of observed series when the exact time of the change is unknown [46]. A version of the Mann–Whitney statistic $U_{t,N}$ is used to test whether two divided segments of a sequence of random variables are from the same population.

Readers may refer to Chen et al. [47] and Xie et al. [48] for a detailed discussion on the Mann–Kendall–Sneyers test and the Pettitt test, respectively.

4.2. Description of SWAT Model. In this paper, the Soil and Water Assessment Tool (SWAT) model was applied to simulate daily streamflow and soil moisture time series in Luanhe River basin. It is a semidistributed, process-based hydrological model. In SWAT model, the watershed is subdivided into Hydrologic Response Units (HRUs), in which runoff generation is simulated by CN method or the Greeen-Ampt infiltration method. The SWAT model has been widely applied to runoff simulation on different time scales.

SWAT-CUP, an automatic parameter estimation method, is used to estimate the parameters in the SWAT model. In SWAT-CUP, algorithm of SUFI-2 is selected to perform calibration and sensitivity analysis. The model performance is assessed by Nash–Sutcliffe model efficiency coefficient (*Ens*) [49] and the coefficient of determination (R^2), calculated as

$$Ens = 1 - \frac{\sum_{i=1}^{n} (O_i - S_i)^2}{\sum_{i=1}^{n} (O_i - \overline{O})^2},$$
$$R^2 = \frac{\left[\sum_{i=1}^{n} (O_i - \overline{O})(S_i - \overline{S})\right]^2}{\sum_{i=1}^{n} (O_i - \overline{O})^2 (S_i - \overline{S})^2}, \quad (1)$$

where S_i and O_i are simulated and observed discharge, respectively. $\overline{O}$ is the average of the observed discharge. In general, monthly *Ens* is deemed satisfactory at >0.5 and daily and monthly R^2 are satisfactory at >0.5 [50].

4.3. Drought Identification. Threshold value method [51] has been widely used for drought definition [52–57], and it was employed to identify drought events in this study.

Firstly, a sensitivity analysis of threshold value to drought event identification was carried out to select a proper threshold for the considered study area. The next step is to calculate threshold value according to the selected percentile of the monthly duration curves. Because monthly threshold series is discrete (a "staircase" pattern), a centered moving average of 30 days is applied to smoothen the threshold values. Subsequently, drought event and its drought characteristics (drought duration; onset and end date of drought; drought deficit volume) can be calculated based on the selected threshold value. In order to assure comparability of drought characteristics, it is crucial to apply the same threshold level (the percentile) in drought propagation studies [14].

A drought event is defined to begin when a variable declines below the predefined threshold and continue until the variable exceeds the threshold [58].

To identify whether the variable x lies in a drought situation on day t, a binary variable δ is represented as the following equation:

$$\delta(t) = \begin{cases} 1, & \text{if } x(t) < \tau(t), \\ 0, & \text{if } x(t) \geq \tau(t), \end{cases} \quad (2)$$

where δ refers to the binary variable and τ is the predefined threshold value.

The duration (Δ_i) of a drought event i can be calculated as

$$\Delta i = \sum_{t=1}^{T} \delta(t) \cdot \Delta t, \tag{3}$$

where T is the total length of the variable x and Δt is the time interval.

$$d(t) = \begin{cases} \tau(t) - x(t), & \text{if } x(t) < \tau(t), \\ 0, & \text{if } x(t) \geq \tau(t), \end{cases} \tag{4}$$

where $d(t)$ is the deviation from threshold value τ on the day t.

$$Di = \sum_{t=1}^{T} d(t) \cdot \Delta t, \tag{5}$$

where D_i refers to the deficit volume of drought event i.

$$d_{i,\max} = \max\left(d1(t), \ldots, d_{\mathrm{T}}(t)\right), \tag{6}$$

where $d_{i,\max}$ is the maximum deviation of drought event i.

The deficit volume is viewed as the most appropriate characteristic to measure severity of drought.

Note that deficit volume (D_i) can only be calculated for flow variables, for example rainfall and streamflow with dimension (mmT^{-1}). Soil moisture is a state variable, similar to groundwater head, thus a measure of storage. The storage coefficient must be known to convert soil moisture into a flow variable. It requires detailed information about the properties of soil layers, which was not available. Therefore, deficit volume cannot be calculated for soil moisture and instead maximum deviation ($d_{i,\max}$) is commonly used to measure severity of drought.

Let DS_i represents the average severity of drought event i, calculated as

$$DS_i = \frac{D_i}{\Delta_i}, \tag{7}$$

where D_i and Δ_i are the deficit volume and duration of drought event i, respectively.

Two restrictions are used for identifying minor droughts according to Hisdal et al. [59]: (1) drought events with duration shorter than 5 days or (2) drought events with a deficit volume less than 0.5% of the maximum deficit volume in all the drought events. To reduce the effect of too much minor droughts, the minor droughts which satisfy the two restrictions were not considered in this study.

4.4. Drought Propagation. Drought propagation is a dynamic process which focuses on the propagation from meteorological droughts to agricultural and/or hydrological droughts. Based on the identified drought events for all drought types in the above section, drought propagation patterns will be determined through the analysis of drought characteristics to answer 2 questions: (1) Does meteorological drought definitely result in agricultural and/or hydrological droughts? (2) Are agricultural and/or hydrological droughts necessarily caused by meteorological drought? Then, the driven factors for drought propagation patterns will be found, and drought propagation equation will be established to explain the drought propagation patterns in the study area.

In this study, 3 different drought propagation patterns were identified. The first one is that only meteorological drought occurs without other drought types following (M).

The second one is the case in which a meteorological drought occurs followed by an agricultural or hydrological drought. In its definition, the maximum lag time of onset from meteorological to agricultural/hydrological drought is 45 days. This drought propagation pattern is termed as agricultural or hydrological drought originated from meteorological drought (M-A/M-H).

If the lag time between agricultural/hydrological drought and its previous meteorological drought is longer than 45 days, it is considered that the agricultural/hydrological drought is not caused by meteorological drought, namely, the third propagation pattern (NM-A/NM-H).

5. Results

5.1. Temporal Changes in Precipitation. In this work, a proper modelling of the hydrological response of the Luanhe River basin is a critical issue which was carried out by SWAT model. The model was calibrated in naturalized conditions and then applied to simulate discharge and soil moisture data for the period 1980~2012, with the purpose of removing human influences. Indeed, this approach relies on the assumption that precipitation pattern remains unchanged over the period 1963~2012. Hence, several statistical methods were employed to verify the stationary precipitation pattern.

Time series of annual precipitation during 1963~2012 over the Luanhe River basin was obtained by using Thiessen polygon technique.

The statistic Z values of MK test with TFPW procedure and Sen's slope estimator (Q_{med}) were calculated for the annual precipitation series, with the values of −0.842 and −0.906, respectively. The results indicated a nonsignificant decreasing trend in the annual precipitation at the significance level $\alpha = 5\%$ ($|Z_{1-\alpha/2}| = 1.96$).

The Mann–Kendall–Sneyers test and the Pettitt test were applied at the confidence level of 95% to detect the change point of the annual precipitation series. From the result of Mann–Kendall–Sneyers test (shown in Figure 2(a)), no intersection of the curves within the confidence intervals indicates the absence of a significant change point for the precipitation series. Together with the Pettitt test result (shown in Figure 2(b)), it is demonstrated abrupt changes in the annual precipitation did not occur from 1963 to 2012.

Based on the above results, the precipitation over the Luanhe River basin is free of significant temporal change, implying stationary precipitation pattern during the period 1963~2012.

5.2. Calibration and Validation of SWAT Model. The period before 1979 is undisturbed by human activities, especially without check dams and reservoir in Luanhe River basin. Therefore years of 1963–1979 are considered as undisturbed

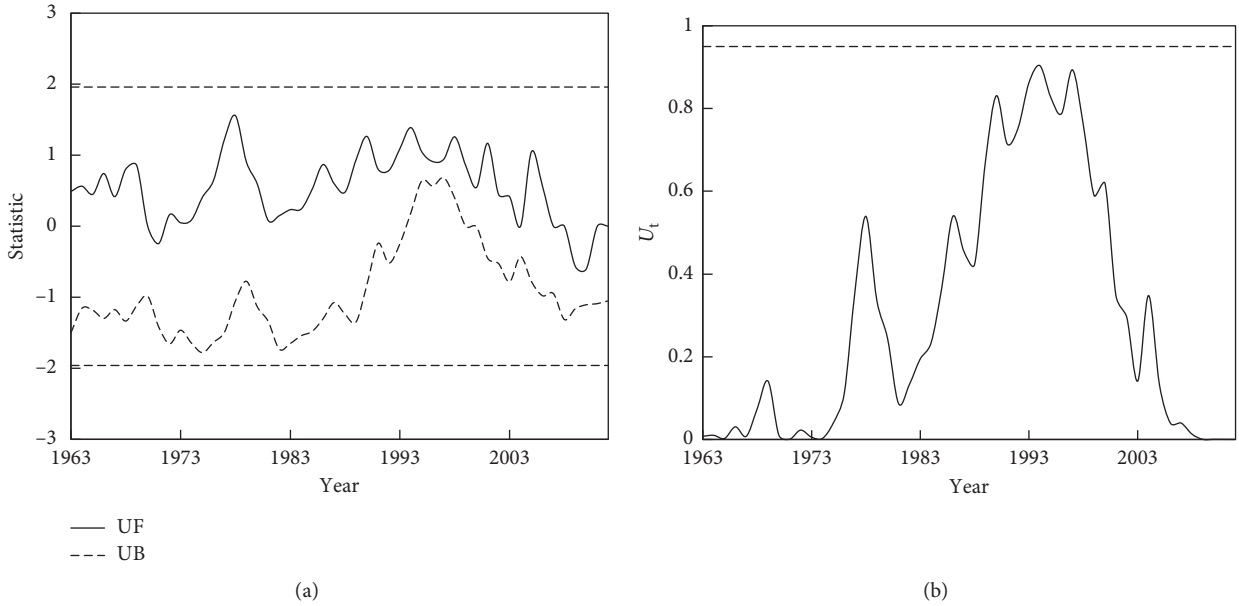

Figure 2: Results of (a) Mann–Kendall–Sneyers test and (b) Pettitt test for the annual precipitation during 1963~2012. The fine dotted lines represent the critical value corresponding to the 95 % confidence level.

period for model calibration and validation based on daily discharges. Runoff data from Luanxian hydrological station are selected to calibrate and validate the SWAT model in the undisturbed period (1963–1979). The results are listed in Table 1. In the calibration period of 1963–1975, *Ens* and R^2 are greater than 0.65 and 0.65, respectively. Especially in monthly simulation, they are both 0.89. In validation period (1976–1979), both *Ens* and R^2 of monthly simulation exceed 0.90, and the values of daily simulation is greater than 0.74. According to Moriasi et al. [50], if the value of *Ens* is greater than 0.50, the SWAT model performs well.

Figure 3 depicts the simulated and observed runoff values on daily scale at Luanxian hydrological station, and it can be seen that the peak of simulated runoff is lower than the measured values, especially in 1964.

For the underestimation of peak flow in model calibration and validation, there might be two major reasons as follows. Firstly, when calibrating the model parameters, more attention was paid on the performance of simulated streamflow processes during dry periods. Secondly, due to the little accumulation of snow during winter, snowmelt made no contribution to the streamflow during spring in the Luanhe River basin. There is no significant snow influence in the basin. Thus, rainfall and its characteristics are the dominant factor driving peak stream flows. However, on account of the limited observed materials available, precipitation data from only 13 rainfall gauge stations were used as the precipitation inputs for SWAT modelling. Accordingly, these limited data could not completely represent the precipitation field of the entire basin. Moreover, with the unevenly distributed precipitation both in space and time, precipitation fields in the Luanhe River basin are spatially variable. As for a rainstorm-generated stormflow event, the model is most unlikely to accurately capture the real center of rainfall, whereupon leading to some deviations existing between the actual and modeled precipitation processes. Consequently, the simulated peak flows showed poor performance.

Figure 4 shows the scatter plot of observed and simulated daily discharge. The low flow is very close to 1 : 1-line, which agrees well with the observed in undisturbed period. Compared with high flow, the model has a good performance to simulate low flow. Hence, this model can be used to simulate discharge without human influences during 1980–2012.

5.3. Drought Characteristics

5.3.1. Sensitivity Analysis of Threshold Value. To evaluate the impact on drought characteristics and select a proper threshold for the study area, the 60th, 70th, 80th, 90th, and 95th percentile of the monthly duration curves were considered to calculate the threshold values, using the observed precipitation data in Luanxian station. According to the different threshold values, 5 sets of meteorological drought events and related characteristics (duration (Δ_i) and deficit volume (D)) were identified. We analyzed and compared the five groups of results for both drought duration and deficit volume. Table 2 summarizes the total number, as well as the average value and standard deviation of $\Delta_i$and D, for the 5 sequences of drought events.

In general, as the percentile decreased, the threshold value increased, leading to the number of drought events rising, as well as the average values of both $\Delta_i$and D. For the too-low threshold value (e.g., the one corresponding to the 95th percentile), most of the defined drought events were essentially extreme events, unexpectedly having too short drought duration and undersize deficit volume. However, for the too-high threshold value (e.g., the one related to the

Table 1: Results of calibration and validation of the River basin.

Luanxian station	Calibration period (1963–1975)		Validation period (1976–1979)	
	Ens	R^2	*Ens*	R^2
Monthly discharge	0.89	0.89	0.96	0.95
Daily discharge	0.66	0.67	0.74	0.76

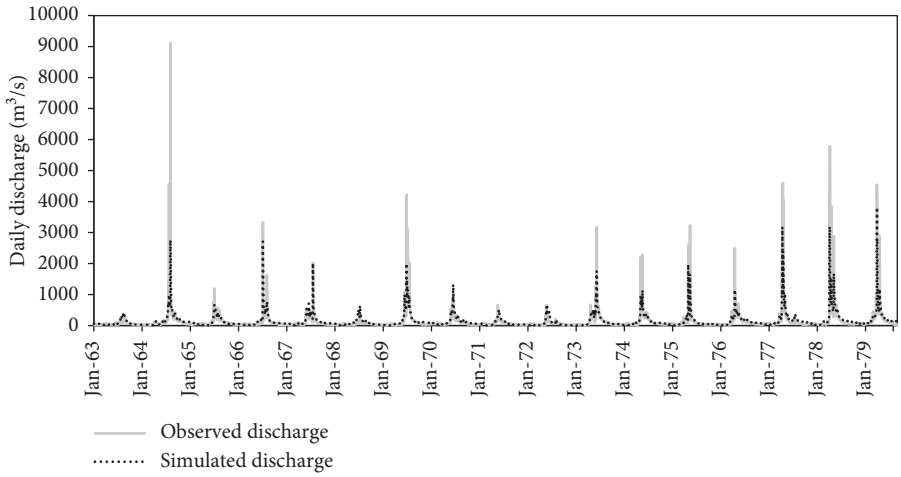

Figure 3: The observed and simulated daily discharge during the undisturbed period (1963–1979).

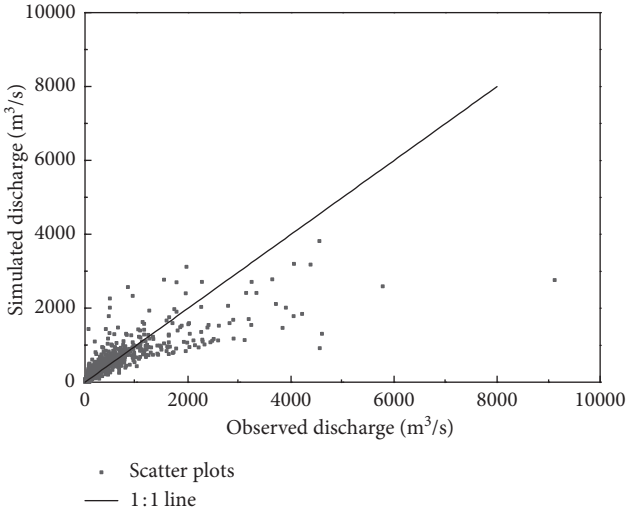

Figure 4: Scatter plots of the daily simulated vs. observed discharge during 1963–1979 at Luanxian station.

60th percentile), extreme drought events were overestimated, and their duration and severity both oversize. In addition, there seemed to be too many small droughts, which is inconsistent with the fact.

As for the 70th, 80th, and 90th percentile, the related 3 sets of drought events had similar average values of drought duration and deficit volume, while the standard deviation descended with the percentile increasing. Several previous studies investigated the features (including drought duration, drought severity, and drought peak) of meteorological droughts in the Luanhe River basin (e.g., Ren et al., Zhou et al., Wang et al., and Wang et al.). By comparing the previous researchers' study results with ours, the drought features defined by the threshold value based on 80th percentile show performance more superior. Consequently, the 80th percentile seems to be applicable to define a proper threshold for the study area. The 80th percentile, locating in the range of 70th to 95th percentile, is often used for perennial rivers [60, 61].

According to Van Loon [14], the same type of threshold is applied to precipitation, runoff, and soil moisture data for the sake of comparison. Therefore, the threshold value was defined as the 80th percentile of the monthly duration curves.

5.3.2. Characteristics of Different Drought Types. According to the simulation results from SWAT model, several characteristics of different drought types were determined. Table 3 shows the characteristics of different drought types. The number of meteorological drought events is obviously the largest, which is 1.4 and 1.5 times larger than hydrological drought and agricultural drought, respectively. However, meteorological droughts have considerably shorter duration, which is about half of agricultural drought on average. From meteorological drought to hydrological drought, the mean deficit volume attenuates considerably.

The longest duration of hydrological drought is more than 200 days, which is comparable to agricultural drought. 80% of drought events are less than 70 days for all drought types. Drought events with less than 30 days account for 74%, 67%, and 66% for meteorological, agricultural, and hydrological drought, respectively.

The largest deficit volume of meteorological and hydrological drought is 44 mm and 10 mm, respectively. 80%

Table 2: Summary of drought characteristics of meteorological drought events based on the 5 different threshold values.

Threshold		Number of single deficits		Drought events	
				Drought duration	Deficit volume
Percentile of observed precipitation	60th	139	Mean	30.15 day	7.01 mm
			SD	11.39	24.89
	70th	134	Mean	25.61 day	5.43 mm
			SD	8.86	19.02
	80th	131	Mean	24.13 day	5.22 mm
			SD	7.48	16.19
	90th	124	Mean	22.25 day	4.49 mm
			SD	7.07	14.87
	95th	112	Mean	17.51 day	3.77 mm
			SD	6.21	14.25

"SD" represents standard deviation.

Table 3: Drought characteristics during the period of 1963–2012.

Drought types	Variables	Number	Mean drought duration (day)	Mean deficit volume (mm)	Maximum deviation (mm)
Meteorological drought	Observed precipitation	131	24.13	5.22	—
Agricultural drought	Simulated soil moisture	85	43.28	—	11.51
Hydrological drought	Simulated streamflow	93	37.63	1.15	—

of meteorological drought events are less than 8.2 mm in deficit volume, and 80% of hydrological drought events are less than 1.67 mm. Deficit volume of drought events is markedly larger for precipitation, and the largest deficit volume is 4 times higher than hydrological drought. The reason is that rainfall is larger and more variable, leading to higher deviation from the threshold [18].

The upper Luanhe River basin is located on the Bashang Plateau, the middle reaches flow through Yanshan Mountains, while the downstream area has relatively flat topography. Due to the complex terrain and uneven distributions of precipitation, the streamflow regimen of the basin is dominated by precipitation. In addition, temperature is playing an increasingly important role under the impact of global warming. Accordingly, not only the agricultural drought caused by soil water deficiency would develop into the hydrological drought caused by lack of streamflow, but also the meteorological drought, which results from precipitation shortage and/or increased evaporation, would directly lead to the hydrological drought. This is the main reason behind our results that the identified agricultural drought events are less than hydrological drought events following Table 3.

5.4. Drought Propagation Patterns

5.4.1. Drought Propagation Types. In general, meteorological drought develops into agricultural drought and then hydrological drought. Based on the previous drought identification, each drought event was determined, and there were 3 different drought propagation patterns (Table 4). 83 out of 131 meteorological droughts developed into agricultural or hydrological drought, which accounts for 63.4% of the total meteorological drought events (M-A/M-H). But not all meteorological droughts develop into agricultural and hydrological drought, which means only meteorological drought occurs, and no other drought types follow (M). 48 out of 131 meteorological droughts belonged to this propagation pattern. The third propagation type is that agricultural or hydrological drought is not caused by meteorological drought (NM-A/NM-H).

Table 4: Drought propagation types.

Drought propagation types	Number of events
M-A/M-H	83
M	48
NM-A/NM-H	45

M means meteorological drought only, M-A/M-H means meteorological drought develops into agricultural and hydrological drought, NM-A/NM-H means no meteorological drought but agricultural and hydrological droughts occur.

Table 5 shows the characteristics of each drought type for different drought propagation patterns. For pattern M, the average duration of meteorological droughts is 25.0 days, and the average deficit of meteorological droughts is 1.9 mm. For those meteorological droughts developing into agricultural or hydrological droughts (M-A/M-H), the average meteorological drought duration are 23.6 days and 22.2 days, and the average meteorological drought deficit are 7.9 mm and 7.6 mm, respectively, which are 4.16 times and 4.00 times larger than those for pattern M. Therefore, severe meteorological droughts are prone to develop into agricultural and hydrological droughts.

As to agricultural drought, M-A propagation pattern has a larger average duration value of 46.7 days than NM-A pattern, which has the similar results with maximum deviation. For hydrological drought, the average duration and deficit are 42.9 days and 1.4 mm, respectively, for M-H pattern, which are larger than NM-H pattern. This demonstrates that meteorological droughts can lead to relatively

Table 5: Drought characteristics for each drought propagation pattern.

Drought type	Drought propagation	Average duration (d)	Average deficit (mm)	Maximum deviation (mm)
Meteorological drought	M	25.0	1.9	—
	M-A/M-H	23.6/22.2	7.9/7.6	—
Agricultural drought	M-A	46.7	—	12.1
	NM-A	34.6	—	10.1
Hydrological drought	M-H	42.9	1.4	—
	NM-H	29.1	0.5	—

severe hydrological droughts. Although there are no meteorological droughts for NM-A and NM-H patterns, which means the daily precipitation is higher than the threshold value, the precipitation is below the multiyear average before the occurrence of agricultural and hydrological droughts for several days.

5.4.2. Lag Time from Meteorological to Agricultural/Hydrological Drought. The onset and end time are two important characteristics for drought events, and the lag time from meteorological to agricultural/hydrological drought can express drought development. Therefore, we selected drought events from M-A/M-H drought propagation type which include meteorological, agricultural, and hydrological droughts occurring concurrently, to calculate the average lag time of onset and end time from meteorological to agricultural/hydrological drought. The results are listed in Table 6.

54% of meteorological drought events lead to agricultural droughts, and then hydrological droughts, and there are 39% drought events for which hydrological droughts started before agricultural droughts. The average lag of onset from meteorological to agricultural and hydrological drought is 21.3 days and 26.8 days, respectively. The average lag of end time from meteorological to agricultural and hydrological drought is 36.6 days and 59.2 days, respectively, in which 48% agricultural droughts ended after hydrological droughts.

Table 6: Lag time from meteorological to agricultural/hydrological drought.

	Lag time for M-A (day)	Lag time for M-H (day)
Onset	21.3	26.8
End time	36.6	59.2

5.5. The Driven Factors of Drought Propagation

5.5.1. From Meteorological Drought to Hydrological Drought. According to the NM-A/NM-H drought propagation patterns, meteorological drought is not the only driven factors for agricultural and hydrological droughts. There must be some other factors affecting the occurrence of agricultural and hydrological drought, i.e., precipitation before the onset of agricultural/hydrological drought, evapotranspiration, and so on [62].

Based on monthly precipitation and runoff data, Wu et al. [63] built a nonlinear relationship between hydrological drought duration and meteorological drought duration and hydrological drought severity and meteorological drought severity, respectively. But they did not consider other factors. In this paper, the following factors are chosen as the driven factors for hydrological drought severity (DS_H): (1) simulated daily evapotranspiration during hydrological drought (E), (2) meteorological drought severity (DS_M), (3) simulated mean soil moisture deficit (SD), and (4) the summation of the difference between the daily precipitation and the long-term average daily precipitation 10 (PD_{10}), 20 (PD_{20}), 30 (PD_{30}), and 40 (PD_{40}) days before hydrological drought. Then the relations between hydrological drought severity and each driven factor was analyzed using Pearson correlation analysis, and the results are shown in Table 7.

It can be seen that SD, DS_M and E are positively related to DS_H significantly, and PD_{10} is negatively correlated with DS_H significantly, but PD_{20}, PD_{30} and PD_{40} are not significant with the significance level of 0.01. With the increase of SD, DS_M and E, together with the decrease of PD_{10}, hydrological drought may occur. Then the relationship between DS_H and each significant driven factor is described by an exponential function, shown in Figure 5.

To further illustrate the drought propagation pattern of M-H and NM-H, the relationship between drought severity (DS_H) and all the driven factors is built using multiple regression analysis, which can be expressed as

$$\begin{aligned} DS_H = {} & 0.011 * \mathrm{EXP}(1.130DS_M + 0.540E \\ & + 0.012\mathrm{SD} - 0.035PD_{10}) - 0.008. \end{aligned} \tag{8}$$

The coefficient of determination (R^2) is 0.656. The calculated DS_H and observed DS_H are plotted in Figure 6. The plots are scattered systematically along the 1:1 line. Therefore, the equation can reflect the comprehensive impacts of the selected driven factors on hydrological drought. The conditions of these 3 propagation types are listed in Table 8.

5.5.2. From Meteorological Drought to Agricultural Drought. Similar to the propagation from meteorological to hydrological drought, some contributing factors affecting agricultural drought severity (SD) are chosen: (1) DS_M, (2) evapotranspiration during agricultural drought (E_A), (3) PD_{10}, PD_{20}, PD_{30}, and PD_{40}. The Pearson correlation coefficients between SD and each contributing factor are listed in Table 9. It can be seen that DS_M, EA, and PD_{10} passed the significance test with the significance level of 0.01. DS_M and EA have a positive impact on agricultural drought,

Table 7: Pearson correlation analysis between hydrological drought severity and each driven factor.

Driven factors	Correlation coefficient	p
SD	0.422	0.0004
DS_M	0.662	0.000000000002
E	0.549	0.00000003
PD_{10}	−0.451	0.00001
PD_{20}	−0.213	0.046
PD_{30}	−0.056	0.604
PD_{40}	−0.032	0.766

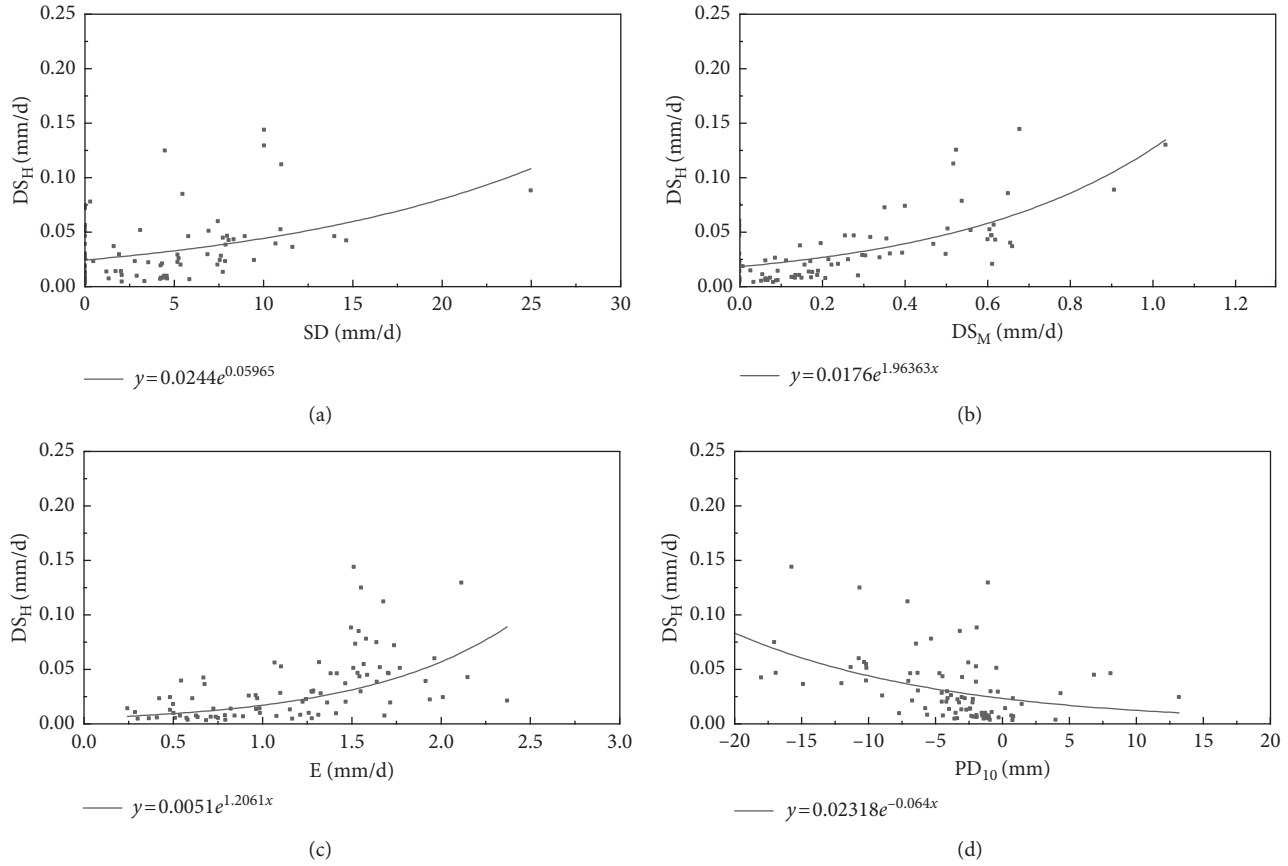

Figure 5: The exponential function between DS_H and SD, DS_M, E PD_{10}.

while PD_{10} has negative impact. We also fitted an exponential function between SD and each driven factor (not shown here). Multiple regression was established for SD and the 3 driven factors, and the model is given as

$$\mathrm{SD} = 16.592 * \mathrm{EXP}\left(0.375\mathrm{DS_M} + 0.084E_A - 0.004\mathrm{PD_{10}}\right) - 15.074. \quad (9)$$

The coefficient of determination of Equation (9) is 0.4. The calculated SD and the observed values are plotted in Figure 7, which scattered near the 1:1 line. This model could explain the drought propagation type of M, M-A, and NM-A. The conditions of the 3 drought propagation types from meteorological to agricultural drought are listed in Table 10.

6. Discussion

This study uses daily rainfall, soil moisture, and runoff data to identify drought propagation patterns. Compared with monthly data, daily data perform better in identifying the drought characteristics (the precise drought onset, duration, end time, and number of drought events). In some previous studies in which monthly data were used, the relations between meteorological drought index and hydrological drought index with l-month ($l = 1, 2, 3\ldots$) lag time were built, and l month with the highest correlation coefficient was considered as the lag time, which was invariant for a given watershed [16, 64, 65]. However, because of different drought characteristics for each drought event, the lag time must be changed from event to event. Drought lag time on the basis of daily data could avoid such a problem.

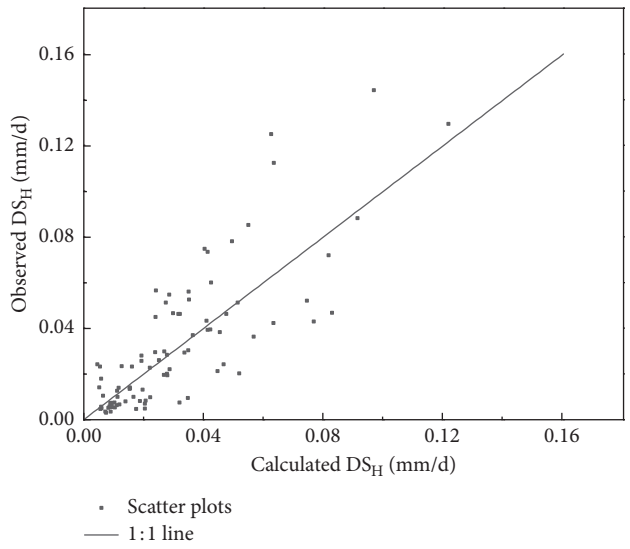

Figure 6: Scatter plots of the calculated DS_H and observed DS_H.

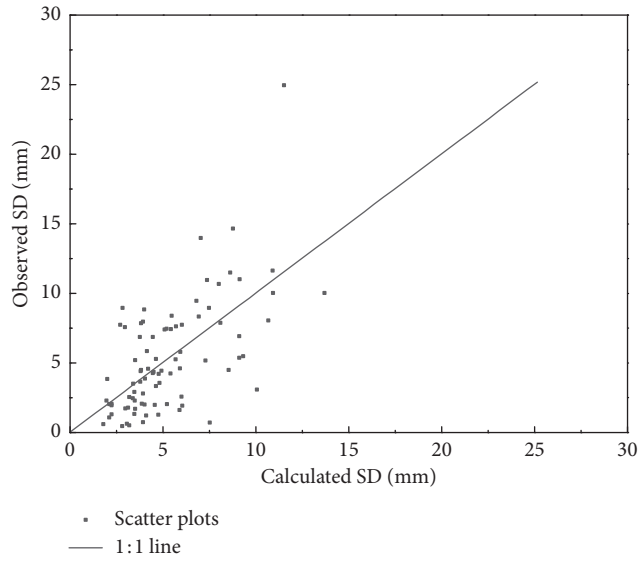

Figure 7: The scatters of simulated and observed SD.

Table 8: The conditions of (M) M-H and NM-H propagation patterns.

Drought propagation pattern	Conditions
M	$DS_M > 0$, $(1.130DS_M + 0.540E + 0.012SD - 0.035PD_{10}) \leq -0.318$
M-H	$DS_M > 0$, $(1.130DS_M + 0.540E + 0.012SD - 0.035PD_{10}) > -0.318$
NM-H	$DS_M = 0$, $(0.540E + 0.012SD - 0.035PD_{10}) > -0.318$

Table 9: Pearson correlation coefficients between SD and the driven factors.

Driven factors	Correlation coefficient	p
DS_M	0.574	$p = 0.00000001$
E_A	0.354	$p = 0.0009$
PD_{10}	−0.264	$p = 0.0053$
PD_{20}	−0.104	$p = 0.3487$
PD_{30}	−0.063	$p = 0.5699$
PD_{40}	−0.093	$p = 0.3979$

To remove the impacts of human activities, we applied the SWAT model to simulate streamflow from 1963 to 2012 under the 1970 land use condition. This concept stemmed from the observation-modelling framework presented by Van Loon and Van Lanen [18]; who applied a conceptual hydrological model of HBV in a case study area in Spain. Because there are no observed soil moisture values in the entire watershed, another advantage by using SWAT is to provide simulated daily soil moisture to identify agricultural droughts. Groundwater system was not considered for hydrological drought in this study, since the data are not available. However, streamflow drought could represent the hydrological drought in many previous studies [66–68]. Thus, rainfall, soil moisture, and streamflow data could be used to analyze drought propagation patterns.

Table 10: The conditions of propagation from meteorological to agricultural drought.

Drought propagation type	Conditions
NM-A	$DS_M = 0$, $(0.084E - 0.004PD_{10}) > -0.095$
M-A	$DS_M > 0$, $(0.375D_M + 0.084E - 0.004PD_{10}) < -0.095$
M	$DS_M > 0$, $(0.375D_M + 0.084E - 0.004PD_{10}) \geq -0.095$

The deficit volume, which was viewed as the best drought characteristic to study drought propagation [58], was not used to calculate for soil moisture storage [14]. Thereby, deficit value was only used to compare meteorological drought and hydrological drought. According to the obtained drought propagation patterns, meteorological drought unnecessarily results in agricultural and hydrological droughts, and vice versa. In order to explain the 3 drought propagation patterns, we tried to find the possible driven factors of the formation of agricultural and hydrological droughts. Then the relations between hydrological drought and the driven factors and between agricultural drought and the driven factors were established with the coefficients of determination 0.656 and 0.4, respectively. Although the accuracy is not high enough to make hydrological or agricultural drought forecast, it indeed interprets drought propagation patterns in the Luanhe river basin.

80th percentile is widely used as the threshold value in drought identification, which was also applicable in the Luanhe River basin [69]. Different threshold value may have impact on drought characteristics and then on drought propagation patterns. And also droughts with duration longer than 5 days were counted and those shorter than 5 days were neglected, which also influenced propagation patterns. Therefore, the uncertainty of the selection of

threshold values and drought events should be further studied. Human activities are not considered here, which is another issue to be studied in the future.

7. Conclusions

This paper contributed to identification of drought propagation patterns in a watershed, and in particular, the explanation through the daily observed and simulated data. The conclusions are as follows:

(1) To remove the impact of human activities and obtain the soil moisture data, SWAT model was employed to get the hydrometeorological data under natural condition. The model performed very well in the Luanhe river basin, and the simulated results could be used for study of drought propagation.

(2) 3 types of drought propagation patterns were obtained, which are M-A/H, M-NA/NH, and NM-A/H. Meteorological drought unnecessarily resulted in agricultural/hydrological drought, and agricultural/hydrological drought was not necessarily caused by meteorological drought.

(3) Possible driven factors of agricultural and hydrological drought were found, and the relations between agricultural/hydrological drought and the driven factors were built by multiple regression method. These relations could explain the 3 drought propagation patterns.

Data Availability

For data confidentiality and privacy, we are prohibited to share the data used for producing the results of this paper.

Conflicts of Interest

The authors declare that they have no conflicts of interest.

Acknowledgments

This work was supported by National Natural Science Foundation of China (no. 51479130). We are grateful to Hydrology and Water Resource Survey Bureau of Hebei Province for providing rainfall data.

References

[1] J. Evans and R. Geerken, "Discrimination between climate and human-induced dryland degradation," *Journal of Arid Environments*, vol. 57, no. 4, pp. 535–554, 2004.

[2] H. A. J. Van Lanen, N. Wanders, L. M. Tallaksen, and A. F. Van Loon, "Hydrological drought across the world: impact of climate and physical catchment structure," *Hydrology and Earth System Sciences*, vol. 17, no. 5, pp. 1715–1732, 2013.

[3] H. Hisdal and L. M. Tallaksen, "Estimation of regional meteorological and hydrological drought characteristics: a case study for Denmark," *Journal of Hydrology*, vol. 281, no. 3, pp. 230–247, 2003.

[4] S. L. Lewis, P. M. Brando, O. L. Phillips, G. M. van der Heijden, and D. Nepstad, "The 2010 amazon drought," *Science*, vol. 331, no. 6017, p. 554, 2011.

[5] M. T. Van Vliet, J. R. Yearsley, F. Ludwig, S. Vögele, D. P. Lettenmaier, and P. Kabat, "Vulnerability of US and European electricity supply to climate change," *Nature Climate Change*, vol. 2, no. 9, pp. 676–681, 2012.

[6] D. A. Wilhite, *Drought: A Global Assessment*, Routledge, Abingdon, United Kingdom, 2000.

[7] L. M. Tallaksen and H. A. J. Van Lanen, *Hydrological Drought. Processes and Estimation Methods for Streamflow and Groundwater*, 2004.

[8] A. F. Van Loon and G. Laaha, "Hydrological drought severity explained by climate and catchment characteristics," *Journal of Hydrology*, vol. 526, pp. 3–14, 2015.

[9] A. K. Mishra and V. P. Singh, "A review of drought concepts," *Journal of Hydrology*, vol. 391, no. 1-2, pp. 202–216, 2010.

[10] S. A. Changnon, *Detecting Drought Conditions in Illinois*, Illinois State Water Survey, Champaign, IL, USA, 1987.

[11] E. A. B. Eltahir and P. J. F. Yeh, "On the asymmetric response of aquifer water level to floods and droughts in Illinois," *Water Resources Research*, vol. 35, no. 4, pp. 1199–1217, 1999.

[12] R. R. Heim, "A review of twentieth-century drought indices used in the United States," *Bulletin of the American Meteorological Society*, vol. 83, no. 8, pp. 1149–1165, 2002.

[13] J. H. Sung and E. S. Chung, "Development of streamflow drought severity– duration– frequency curves using the threshold level method," *Hydrology and Earth System Sciences*, vol. 18, no. 9, pp. 3341–3351, 2014.

[14] A. F. Van Loon, *On the Propagation of Drought: How Climate and Catchment Characteristics Influence Hydrological Drought Development and Recovery*, 2013.

[15] H. A. Van Lanen, *Drought Propagation through the Hydrological Cycle*, Vol. 308, IAHS publication, Wallingford, UK, 2006.

[16] S. Huang, P. Li, Q. Huang, G. Leng, B. Hou, and L. Ma, "The propagation from meteorological to hydrological drought and its potential influence factors," *Journal of Hydrology*, vol. 547, pp. 184–195, 2017.

[17] A. F. Van Loon, E. Tijdeman, N. Wanders, H. A. J. Van Lanen, A. J. Teuling, and R. Uijlenhoet, "How climate seasonality modifies drought duration and deficit," *Journal of Geophysical Research: Atmospheres*, vol. 119, no. 8, pp. 4640–4656, 2014.

[18] A. F. Van Loon and H. A. J. Van Lanen, "A process-based typology of hydrological drought," *Hydrology and Earth System Sciences*, vol. 16, no. 7, pp. 1915–1946, 2012.

[19] B. Beyene, "Drought classification, propagation analysis, and prediction of anomalies," Technical Report, 2015.

[20] L. M. Tallaksen, H. Hisdal, and H. A. J. Van Lanen, "Space–time modelling of catchment scale drought characteristics," *Journal of Hydrology*, vol. 375, no. 3-4, pp. 363–372, 2009.

[21] L. J. Barker, J. Hannaford, A. Chiverton, and C. Svensson, "From meteorological to hydrological drought using standardised indicators," *Hydrology and Earth System Sciences*, vol. 20, no. 6, pp. 2483–2505, 2016.

[22] X. Ye, X. Li, C.-Y. Xu, and Q. Zhang, "Similarity, difference and correlation of meteorological and hydrological drought indices in a humid climate region–the Poyang Lake catchment in China," *Hydrology Research*, vol. 47, no. 6, pp. 1211–1223, 2016.

[23] R. Pandey, S. Mishra, R. Singh, and K. Ramasastri, "Streamflow drought severity analysis of Betwa river system (INDIA)," *Water resources management*, vol. 22, no. 8, pp. 1127–1141, 2008.

[24] D. Tigkas, H. Vangelis, and G. Tsakiris, "Drought and climatic change impact on streamflow in small watersheds," *Science of the Total Environment*, vol. 440, pp. 33–41, 2012.

[25] E. Tijdeman, A. Van Loon, N. Wanders, and H. Van Lanen, "The effect of climate on droughts and their propagation in different parts of the hydrological cycle," Technical Report EU Drought R&SPI Project, no. 2, pp. 1–70, 2012.

[26] M. Van Huijgevoort, P. Hazenberg, H. Van Lanen, and R. Uijlenhoet, "A generic method for hydrological drought identification across different climate regions," *Hydrology and Earth System Sciences*, vol. 16, no. 8, p. 2437, 2012.

[27] H. Wu, L.-K. Soh, A. Samal, and X.-H. Chen, "Trend analysis of streamflow drought events in Nebraska," *Water Resources Management*, vol. 22, no. 2, pp. 145–164, 2008.

[28] G. A. Corzo Perez, M. H. J. van Huijgevoort, F. Voß, and H. A. J. Van Lanen, "On the spatio-temporal analysis of hydrological droughts from global hydrological models," *Hydrology and Earth System Sciences*, vol. 15, no. 9, pp. 2963–2978, 2011.

[29] A. Fleig, *Hydrological Drought–a Comparative Study Using Daily Discharge Series from Around The World*, Institut für Hydrologie der Albert-Ludwigs-Universität Freiburg i, Br., 144s, Freiburg, Germany, 2004.

[30] L. M. Tallaksen et al., *Propagation of Drought in a Groundwater Fed Catchment, the Pang in the UK*, IAHS Publication, Wallingford, UK, 2006.

[31] Y. Jiang, C. Liu, X. Li, L. Liu, and H. Wang, "Rainfall-runoff modeling, parameter estimation and sensitivity analysis in a semiarid catchment," *Environmental Modelling & Software*, vol. 67, pp. 72–88, 2015.

[32] G. Fischer et al., *Global Agro-cological Zones Assessment for Agriculture (GAEZ 2008)*, IIASA, Laxenburg, Austria and FAO, Rome, Italy, 2008.

[33] F. Nachtergaele et al., *Harmonized world soil database (Version 1.0), Food and Agric Organization of the UN (FAO)*, International Inst. for Applied Systems Analysis (IIASA), ISRIC-World Soil Information, Inst of Soil Science-Chinese Acad of Sciences (ISS-CAS); EC-Joint Research Centre (JRC), 2008.

[34] M. G. Kendall, *Rank Correlation Methods*, Griffin, London, UK, 1975.

[35] H. B. Mann, "Nonparametric tests against trend," *Econometrica*, vol. 13, no. 3, pp. 245–259, 1945.

[36] S. Yue, P. Pilon, B. Phinney, and G. Cavadias, "The influence of autocorrelation on the ability to detect trend in hydrological series," *Hydrological Processes*, vol. 16, no. 9, pp. 1807–1829, 2002.

[37] P. K. Sen, "Estimates of the regression coefficient based on Kendall's tau," *Journal of the American Statistical Association*, vol. 63, pp. 1379–1389, 1968.

[38] R. O. Gilbert, *Statistical Methods for Environmental Pollution Monitoring*, pp. 204–208, Van Nostrand Reinhold Company, New York, NY, USA, 1987.

[39] M. R. Kousari, H. Ahani, and R. Hendi-zadeh, "Temporal and spatial trenddetection of maximum air temperature in Iran during 1960-2005," *Global and Planetary Change*, vol. 111, pp. 97–110, 2013.

[40] O. Kisi and M. Ay, "Comparison of Mann–Kendall and innovative trend method for water quality parameters of the Kizilirmak River, Turkey," *Journal of Hydrology*, vol. 513, pp. 362–375, 2014.

[41] R. M. Da Silva, C. A. Santos, M. Moreira, J. Corte-Real, V. C. Silva, and I. C. Medeiros, "Rainfall and river flow trends using Mann–Kendall and Sen's slope estimator statistical tests in the Cobres River basin," *Natural Hazards*, vol. 77, no. 2, pp. 1205–1221, 2015.

[42] G. C. Chen, "Slide F test of change-point analysis," *Journal of China Hydrology*, 2006, in Chinese with English abstract.

[43] A. L. Yan, Q. Huang, Z. Liu et al., "Complicated property of runoff time series studied with R/S method," *Journal of Applied Sciences*, vol. 25, no. 2, pp. 214–217, 2007.

[44] L. H. Xiong and S. L. Guo, "Trend test and change-point detection for the annual discharge series of the Yangtze River at the Yichang hydrological station," *Hydrological Sciences Journal*, vol. 49, no. 1, pp. 99–112, 2004.

[45] R. Sneyers, *Sur l'analyse Statistique des Séries d'observations, O.M.M., Note Technique, No 143*, Gencve, Suisse, 1975.

[46] A. N. Pettitt, "A non-parametric approach to the change-point problem," *Applied Statistics*, vol. 28, no. 2, pp. 126–135, 1979.

[47] Z. Chen, Y. Chen, and B. Li, "Quantifying the effects of climate variability and human activities on runoff for Kaidu River Basin in arid region of northwest China," *Theoretical & Applied Climatology*, vol. 111, no. 3-4, pp. 537–545, 2013.

[48] H. Xie, D. Li, and L. Xiong, "Exploring the ability of the Pettitt method for detecting change point by Monte Carlo simulation," *Stochastic Environmental Research & Risk Assessment*, vol. 28, no. 7, pp. 1643–1655, 2014.

[49] J. E. Nash and J. V. Sutcliffe, "River flow forecasting through conceptual models part I—A discussion of principles," *Journal of hydrology*, vol. 10, no. 3, pp. 282–290, 1970.

[50] D. N. Moriasi, J. G. Arnold, M. W. Van Liew, R. L. Bingner, R. D. Harmel, and T. L. Veith, "Model evaluation guidelines for systematic quantification of accuracy in watershed simulations," *Transactions of the ASABE*, vol. 50, no. 3, pp. 885–900, 2007.

[51] V. Yevjevich, "An objective approach to definitions and investigations of continental hydrologic droughts, hydrology paper 23, Colorado State University, Fort Collins, Colorado," *Journal of Hydrology*, vol. 7, no. 3, 1967.

[52] B. Bonaccorso, A. Cancelliere, and G. Rossi, "An analytical formulation of return period of drought severity," *Stochastic Environmental Research and Risk Assessment*, vol. 17, no. 3, pp. 157–174, 2003.

[53] B. Bonaccorso, D. J. Peres, A. Cancelliere, and G. Rossi, "Large scale probabilistic drought characterization over Europe," *Water Resources Management*, vol. 27, no. 6, pp. 1675–1692, 2013.

[54] A. Cancelliere and J. D. Salas, "Drought length properties for periodic-stochastic hydrologic data," *Water Resources Research*, vol. 40, no. 2, pp. 389–391, 2004.

[55] A. Cancelliere and J. D. Salas, "Drought probabilities and return period for annual streamflows series," *Journal of Hydrology*, vol. 391, no. 1-2, pp. 77–89, 2010.

[56] B. Fernández and J. D. Salas, "Return period and risk of hydrologic events," *Journal of Hydrologic Engineering*, vol. 4, no. 4, pp. 308–316, 1999.

[57] J. D. Salas, C. Fu, A. Cancelliere et al., "Characterizing the severity and risk of drought in the Poudre River, Colorado," *Journal of Water Resources Planning and Management*, vol. 131, no. 5, pp. 383–393, 2005.

[58] B. Heudorfer and K. Stahl, "Comparison of different threshold level methods for drought propagation analysis in Germany," *Hydrology Research*, vol. 48, no. 5, pp. 1311–1326, 2016.

[59] H. Hisdal, L. M. Tallaksen, B. Clausen, E. Peters, and A. Gustard, "5 hydrological drought characteristics," *Developments in Water Science*, vol. 4, 2004.

[60] F. Chen and J. Li, "Quantifying drought and water scarcity: a case study in the Luanhe river basin," *Natural Hazards*, vol. 81, no. 3, pp. 1913–1927, 2016.

[61] T. R. Kjeldsen, A. Lundorf, and D. Rosbjerg, "Use of a two-component exponential distribution in partial duration modelling of hydrological droughts in Zimbabwean rivers," *Hydrological Sciences Journal*, vol. 45, no. 2, pp. 285–298, 2000.

[62] Wang et al., *Summarized the Features of Drought Propagation, and Pointed out that Analyzing the Mechanisms of Drought Propagation Quantitatively were Needed to be further Investigated*, 2016.

[63] J. Wu, X. Chen, H. Yao et al., "Non-linear relationship of hydrological drought responding to meteorological drought and impact of a large reservoir," *Journal of Hydrology*, vol. 551, pp. 495–507, 2017.

[64] J. Z. Li, S. H. Zhou, and R. Hu, "Hydrological drought class transition using SPI and SRI time series by loglinear regression," *Water Resources Management*, vol. 30, no. 2, pp. 669–684, 2016.

[65] I. Nalbantis and G. Tsakiris, "Assessment of hydrological drought revisited," *Water Resources Management*, vol. 23, no. 5, pp. 881–897, 2009.

[66] F. Luc and D. Rutger, "Impact of global warming on streamflow drought in Europe," *Journal of Geophysical Research: Atmospheres*, vol. 114, no. D17, pp. 767–773, 2009.

[67] H. B. Donald, W. Jeremy, and D. V. Bonin, "An integrated approach to the estimation of streamflow drought quantiles," *Hydrological Sciences Journal*, vol. 49, no. 6, pp. 1011–1024, 2009.

[68] B. Coulthard, D. J. Smith, and D. M. Meko, "Is worst-case scenario streamflow drought underestimated in British Columbia? A multi-century perspective for the south coast, derived from tree-rings," *Journal of Hydrology*, vol. 534, pp. 205–218, 2016.

[69] S. H. Zhou, *Research on the Streamflow Change and the Distinction of Hydrological Drought in Luanhe River Basin*, Tianjin University, Tianjin, China, 2015.